

Theory and experiment on optical bistability in a Fabry-Perot interferometer with an intracavity nematic liquid-crystal film

I. C. Khoo and J. Y. Hou*

Department of Physics and Astronomy, Wayne State University, Detroit, Michigan 48202

R. Normandin and V. C. Y. So

Division of Physics, National Research Council of Canada, Ottawa, Canada K1A 0R6

(Received 2 February 1983)

We have studied theoretically and experimentally the nonlinear Fabry-Perot transmission of a cavity with a thin nematic liquid-crystal film. Various modes of operation have been observed, using a moderate-power cw laser. In the limit of small reorientation angles, the optically induced molecular reorientation of the birefringent crystal and the nonlinear phase shift is solved for a homeotropically aligned crystal. Multiple-valued Fabry-Perot transmission is obtained by solving the nonlinear equations that couple the optical phase shift with the cavity transmission. The time-independent nature of the process and the explicit quantitative expressions involving the nematic liquid-crystal parameters allow a direct comparison between the theory and experimental results. Good quantitative agreement is demonstrated.

I. INTRODUCTION

Optical bistability has been a subject of intensive investigation because of its significance in fundamental and applied problems.¹⁻⁶ There are several basic mechanisms for optical bistability. Perhaps the most commonly employed is a Fabry-Perot interferometer with an intracavity nonlinear medium (i.e., a medium that possesses an intensity-dependent refractive index). Depending on the relative magnitude of the medium's response time versus the cavity time and the laser, the response (i.e., transmission) of the system may be classified into the time-dependent (transient, and quasisteady state) and the time-independent steady-state regimes. Earlier work by Shen and co-worker⁵ and more recently Gibb's *et al.*⁶ have dealt with the time-dependent problem in several contexts. Interesting transient or oscillatory behaviors below and above the switching has been predicted and observed, even in the steady-state case involving a cw laser. When the medium response time is very much longer than all the relevant characteristic times, the system's behavior under a cw laser illumination no longer has these complicating features. Consequently, one would expect that the output characteristics of the Fabry-Perot can be studied in a clear-cut way, linking the medium's characteristics with the Fabry-Perot transmission without the time variable.

For a nonlinear Fabry-Perot interferometer action to occur under cw laser illumination (typically in the

watts power range), the nonlinearity of the medium must be unusually high. A well-tested system is Na vapor, with the dye laser tuned to the *D* lines. The underlying nonlinearity is the intensity-dependent index associated with the optical absorption. A nonabsorptive case was recently demonstrated, where the nonlinearity is the optical-field-induced molecular reorientation of an aligned (birefringent) nematic liquid-crystal film.⁷

In the work by Bischoffberger and Shen, liquid crystals in the *isotropic* (liquid) phase were used. The nonlinearity in this phase is rather small (typically of the order of or a few times larger than those observed in well-known nonlinear liquids like CS₂) and consequently a pulsed laser has to be used. The various modes of operation (differential gain, bistability, etc.) have to be inferred indirectly from the observed time evolution of the pulsed laser used. Our preliminary results⁷ have shown that a 50- μ m (or so) thick nematic liquid-crystal film can provide a sufficient optical phase shift in a Fabry-Perot cavity, for the direct observation of various modes of transmission operations using a moderately powered cw laser. Although the response times of nematics are generally too slow for a switching application, they are useful for wave-front conjugation involving two counterpropagating beams where speed is not a particularly important consideration. Another useful (obvious) feature is the frequency independence of the underlying molecular reorientation process, so that conceivably other types of laser (besides the

argon-ion laser to be discussed below) may be used for specific problems. These considerations motivate the present detailed theoretical analysis. The detailed electrodynamic for a birefringent crystal involving active optical responses (i.e., nonlinearity) as presented here will be useful in other studies. It is also found that the experimental results agree very well with the theory.

We first review in Sec. II the theory of liquid-crystal molecular reorientation by two counter propagating optical beams, and derive expressions for the optically induced refractive index change as a function of the crystal's parameter. In Sec. III, the optical Fabry-Perot system is described and expressions for the output and other optical quantities are obtained. In Sec. IV the experimental setup for the Fabry-Perot transmission characteristics and the experimental results are presented and compared with the theory.

II. THEORY—LIQUID-CRYSTAL CHARACTERISTICS

Consider a homotropically aligned nematic liquid-crystal film situated inside a Fabry-Perot cavity, as depicted schematically in Fig. 1. The light propagation vectors and the phase propagation vector \hat{k} make angles β_2 and β_1 with \hat{n} , the director axis which points along z . The total optical field inside the nematic may be represented as the sum of a forward propagating field $E_{0f}\exp[-i\psi(x,z)]$ and a backward propagating wave $E_{0b}\exp\{i[\psi(x,z)-\psi_0]\}$, where ψ_0 is the phase associated with the propagation in the space between the film and M_2 . For simplicity we assume all the losses due to reflection may be concentrated at the two boundary glass slides of the liquid-crystal film and exposed by $\sqrt{G}\sqrt{G}$, so E_{0b} is related to E_{0f} by $E_{0b}^2 = E_{0f}^2 GR$, where R is the reflectance of the mirror M_2 and \sqrt{G} the transmittance of the glass slide.

The total optical field inside the nematic is therefore given by

$$E_{0p}^2(z) = E_{0f}^2 + E_{0b}^2 + 2E_{0f}E_{0b}\cos[2\psi(x,z) - \psi_0]. \quad (1)$$

The equation governing the reorientation of the director axis of the nematic is obtained by a minimization of the free energy F of the system,

$$F = \frac{1}{2}K \left[\frac{\partial\theta}{\partial z} \right]^2 - \frac{\Delta\epsilon}{8\pi} E_{0p}^2 \cos^2(\theta + \beta_2), \quad (2)$$

where K is the elastic constant (for bending), $\Delta\epsilon$ is

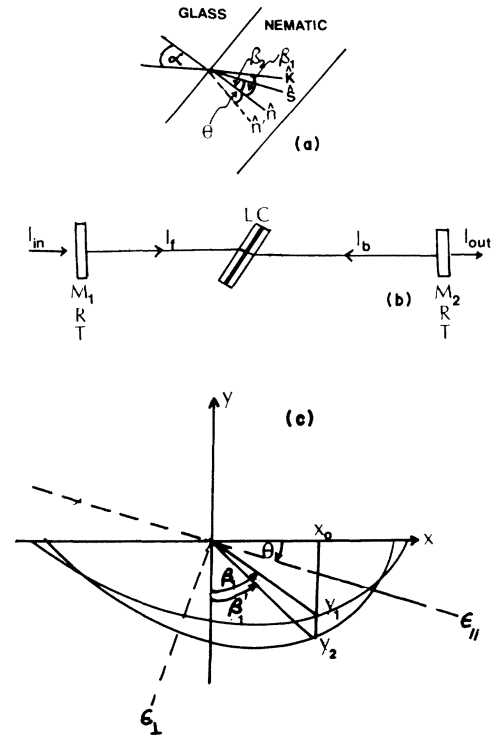


FIG. 1. (a) Schematics of the optical-field propagation in the homeotropically aligned nematic liquid crystal. $\hat{n} = \hat{z}$ is normal to the plane of the boundary glass plates. \hat{S} is Poynting's vector and \hat{k} the phase propagation vector. \hat{n}' is the reoriented direction of the director axis. α is the angle of incidence from the glass to the nematic. (b) Schematic of the Fabry-Perot cavity. M_1 and M_2 are mirrors. I_i is the incident laser intensity I_f is the forward propagating and I_b , the backward propagating beam intensity. (c) Refractive index ellipse for calculation of the refractive index of the nematic for an extraordinary ray. $x_0 = \sin\alpha$, $v_i = n(\beta_i)\cos\beta_i$.

the dielectric anisotropy ($\Delta\epsilon = \epsilon_{||} - \epsilon_{\perp}$, where $\epsilon_{||}$ and ϵ_{\perp} are the dielectric constant for optical field polarized parallel and perpendicular to the director axis, respectively). The minimization procedure gives a torque balance equation

$$K \frac{\partial^2\theta}{\partial z^2} - \frac{\Delta\epsilon}{8\pi} E_{0p}^2 \sin 2(\beta_2 + \theta) = 0. \quad (3)$$

We now make a simplification (which can be justified as we shall presently see) of assuming that θ is small. This assumption has been made in other calculations and was shown to be valid for an applied optical field below the so-called optical Freedericksz field.⁸ Typically, the optical Freedericksz field for a 50- μm (or so) thick nematic crystal corresponds to an intensity on the order of 10^3 W/cm^2 , whereas the

optical intensity to be used in these nonlinear Fabry-Perot experiments will be on the order of at most 10^2 W/cm². Furthermore, we know from pre-

vious calculations, that θ is proportional to $\sin 2\beta_2$ and $\theta \ll \beta_2$ (i.e., $\beta_2 + \theta \approx \beta_2$). Thus Eq. (3) can be simplified to give

$$K \frac{\partial^2 \theta}{\partial z^2} = \frac{\Delta \epsilon}{8\pi} E_{0f}^2 [1 + GR + 2\sqrt{GR} \cos(2k_z z + 2k_x x - \phi_0)] \sin 2\beta_2. \quad (4)$$

Writing

$$\theta_1 = 2K\theta \left[\frac{\Delta \epsilon}{8\pi} E_{0f}^2 \sin(2\beta_2)(1 + GR) \right]^{-1},$$

we get

$$\theta_1 = z^2 + bz - \frac{A}{k_z^2} [\cos(2k_z z + 2k_x x) - \cos(2k_x x)], \quad (5)$$

where $A = 4\sqrt{GR}/(1 + GR)$. The solution for θ satisfies the hard boundary condition, i.e., $\theta = 0$ at $z = 0$ and is also equal to 0 at $z = d$. This gives

$$1 + \frac{b}{d} - \frac{A}{(dk_z)^2} [\cos(2k_z z + 3k_x x) - \cos(2k_x x)] = 0. \quad (6)$$

We note here that $dk_z \gg 1$. This means

$$\frac{A}{(dk_z)^2} [\cos(2k_z z + 2k_x x) - \cos(2k_x x)] \ll 1$$

and therefore we have for all intents and purposes $b = -d$. Finally we get

$$\theta(z) = \frac{(1 + GR)E_{0f}^2 \sin(2\beta_2)(z^2 - dz)}{16\pi K}. \quad (7)$$

Consider now the variation of the round-trip phase shift due to the reorientation effect. The round-trip phase shift increment due to the insertion of a liquid-crystal film (without reorientation effect) is

$$\Delta\phi = \frac{4\pi}{\lambda} [\cos\alpha - n(\beta_1)\cos\beta_1]d, \quad (8)$$

where α and β_1 are depicted in Fig. 1(b). The change due to the reorientation effect is depicted by the diagram of refractive index ellipse in Fig. 1(c), where the axis $y = n(\beta)\cos\beta$, $X_0 = \sin\alpha$ is the incident beam angle. The quantity y_1 refers to the case without reorientation while y_2 is for the case with reorientation.

The equation for the refraction index ellipse is thus given by

$$\epsilon_{\perp}(x^2 \cos^2 \theta + y^2 \sin^2 \theta - xy \sin 2\theta) + \epsilon_{\parallel}(x^2 \sin^2 \theta + y^2 \cos^2 \theta + xy \sin 2\theta) = \epsilon_{\perp} \epsilon_{\parallel}, \quad (9)$$

since $x = x_0 = \sin\alpha$ is a constant. The equation for y can be solved to give

$$y = \frac{-x_0 \Delta \epsilon \sin 2\theta \pm [(x_0 \Delta \epsilon \sin^2 \theta)^2 - 4x_0^2 (\epsilon_{\parallel} - \Delta \epsilon \sin^2 \theta)(\epsilon_{\parallel} - \Delta \epsilon \cos^2 \theta - \epsilon_{\perp} \epsilon_{\parallel})]^{1/2}}{2(\epsilon_{\parallel} - \Delta \epsilon \sin^2 \theta)^{1/2}}. \quad (10)$$

Since θ is very small, we can take the approximation of $\sin\theta = \theta$ and neglect the terms associated with θ^2 .

We get

$$y_2 - y_1 = \frac{x_0 \Delta \epsilon \theta}{\epsilon_{\parallel}} = \frac{\sin\alpha \Delta \epsilon \theta}{\epsilon_{\parallel}}. \quad (11)$$

So the increment of phase shift due to reorientation effect is

$$\delta\Phi = \frac{4\pi}{\lambda} \frac{\sin\alpha \Delta \epsilon}{\epsilon_{\parallel}} \int_0^d \theta(z) dz, \quad (12)$$

where $\theta(z)$ is given in Eq. (7). Inserting (7) into (12), we get

$$\delta\Phi = \frac{d^3 \sin\alpha (\Delta \epsilon)^2}{24K \lambda \epsilon_{\parallel}} (1 + GR) \sin(2\beta_2) E_{0f}^2. \quad (13)$$

We have, throughout the analysis, distinguished between the \hat{k} and \hat{s} propagation vectors and denote the angles by β_1 and β_2 , respectively. This is in accordance with optical propagation in a birefringent crystal. In the numerical analysis, however, there is very little difference between using $\sin^2 \beta_1$ or $\sin^2 \beta_2$.

III. FABRY-PEROT CHARACTERISTICS

We now define the following quantities for the Fabry-Perot interferometer. Let η be the total transmittance of the interferometer, i.e., $\eta = I_0/I_i$, where I_0 is the intensity of output beam and I_i is the intensity of incident beam. From the well-known theory of Fabry-Perot interferometer (using a plane-wave approximation)

$$\eta = \frac{\eta_{\max}}{1 + F' \sin^2 \left[\frac{\phi_0 + \delta\Phi}{2} \right]}, \quad (14)$$

where $\eta_{\max} = T^2G/(1-GR)^2$ and $F' = 4GR/(1-GR)^2$, T is the transmittance of mirrors.

The intensity of forward light beam in the liquid-crystal I_{of} is related to the total transmittance η and the incident beam intensity I_i . It is easy to show that

$$I_{of} = \frac{\eta I_i \cos\alpha}{T\sqrt{G} \cos\beta_2}. \quad (15)$$

The relationship between I and E in the thin liquid-crystal film may be obtained as follows. The density of electrical field energy is given by

$$\frac{\vec{E} \cdot \vec{D}}{8\pi} = \frac{E^2}{8\pi} (\epsilon_{\perp} \cos^2\beta_2 + \epsilon_{\parallel} \sin^2\beta_2). \quad (16)$$

On the other hand, we may write

$$\begin{aligned} \frac{\vec{E} \cdot \vec{D}}{8\pi} &= \frac{\vec{E}}{8\pi} \cdot \frac{n}{c} \left[\vec{H} \times \frac{\vec{k}}{k} \right] \\ &= \frac{n}{c} \frac{\vec{k}}{\vec{k}} \cdot \left[\frac{\vec{E} \times \vec{H}}{8\pi} \right] \\ &= \frac{n}{c} \left[\frac{\vec{k} \cdot \vec{S}}{ks} \right] I. \end{aligned} \quad (17)$$

The intensity of the field I is equal to S , while n denotes the extraordinary ray refractive index. Consider the factor $n(\vec{k} \cdot \vec{s})/ks = n'$,

$$\begin{aligned} n' &= \frac{n \vec{k} \cdot \vec{s}}{ks} = \frac{n \vec{D} \cdot \vec{E}}{DE} \\ &= \frac{n(\epsilon_{\parallel} - \Delta\epsilon \sin^2\alpha)}{[\epsilon_{\parallel}^2 - (\epsilon_{\parallel}^2 - \epsilon_{\perp}^2) \sin^2\alpha]^{1/2}}. \end{aligned} \quad (18)$$

Finally, combining (18) with (17) and inserting it into (16), we get

$$E_{of}^2 = \frac{8\pi I_{of} n'}{(\epsilon_{\perp} \cos^2\beta_2 + \epsilon_{\parallel} \sin^2\beta_2) c}. \quad (19)$$

Using I_{of} given by (15) in (19), we get

$$E_{of}^2 = \frac{8\pi\eta n' \cos\alpha I_i}{T\sqrt{G} c (\cos\beta_2)(\epsilon_{\parallel} - \Delta\epsilon \cos^2\beta_2)}. \quad (20)$$

Combining Eq. (24) with (17) we get

$$\delta\Phi = \frac{\eta\pi d^3 n' I_i (1+GR) \sin\alpha \cos\alpha \sin 2\beta_2 (\Delta\epsilon)^2}{3K\lambda\epsilon_{\parallel} T\sqrt{G} c (\cos\beta_2)(\epsilon_{\parallel} - \Delta\epsilon \cos^2\beta_2)} \quad (21)$$

or

$$\eta = \frac{\delta\Phi 3K\lambda\epsilon_{\parallel} T\sqrt{G} c (\epsilon_{\parallel} - \Delta\epsilon \cos^2\beta_2)}{2\pi d^3 n' (\Delta\epsilon)^2 I_i (1+GR) \sin\alpha \cos\alpha \sin\beta_2}. \quad (22)$$

Equations (22) and (14) are the basic equations describing the nonlinear Fabry-Perot transmission characteristics. The numerical calculation is performed using a minicomputer.

The preceding detailed analysis brings out one particular feature of propagation through a nematic liquid-crystal film, namely its birefringent character, and the associated complicated dependence on the geometry (cf. angles α , β_1 , β' , etc.). It is important to note from the rather involved expressions, however, the fact that (a) the nonlinearity of the film [Eq. (13) for the phase shift] increases rapidly with the thickness of the film and (b) the nonlinearity is proportional to $\sin 2\beta_2$ so that for $\beta_2=0$ (normal incidence), there should not be any reorientation induced phase shift (and effects). From this latter observation we can also find out the role played by thermal effect in the nonlinear Fabry-Perot action. It is well known that the refractive index of the liquid crystal (and therefore the phase shift) is dependent on the temperature. For the geometry depicted in Fig. 1, the thermal contribution (associated with a ΔT rise in temperature) is given by

$$\begin{aligned} \Delta n(\Delta T) &= \Delta n_{\parallel}(\Delta T) \sin^2\beta_2 + n_{\perp}(\Delta T) \cos^2\beta_2 \\ &= \Delta n_{\perp}(\Delta T) [1 - (\delta+1) \sin^2\beta_2], \end{aligned} \quad (23)$$

where we have defined

$$\delta \equiv \frac{\Delta n_{\parallel}(\Delta T)}{\Delta n_{\perp}(\Delta T)}. \quad (24)$$

By repeating the (nonlinear Fabry-Perot) experiment for $\beta_2=0$ and $\beta_2 \neq 0$, we can thus deduce the role of thermal effect. It is perhaps appropriate to comment here that for the liquid-crystal 4-cyano-4'-(*n*-pentyl)biphenyl (PCB) used in this experiment, the molecular reorientation mechanism predominates.

IV. EXPERIMENT SETUP

The experimental setup is shown in Fig. 2. The 5145-Å line of the argon-ion laser was narrowed by an intracavity etalon. Its optical power was varied using a half-wave plate and a linear polarizer. Maximum power of the laser was about 1 W, where single mode operation was still maintained. Because of the rather large distance between the laser and the Fabry-Perot setup, the laser beam had diverged considerably at the entrance part of the interferometer. Consequently, it was found to be necessary to use a 37-cm focal-length lens to lightly recollimate the beam. The resulting beam intensity distribution in the Fabry-Perot was found to resemble that obtained from an extended source, i.e., concentric interference rings maxima and minima are obtained. As the phase of the Fabry-Perot was changed by a computer-controlled piezoelectric transducer mounted on the entrance mirror, these bright and dark rings are shifted. Using two pinholes after the exit window, the intensity of the center spot was monitored. The measured finesse of the system was about 4. This is consistent with the 90% reflecting mirrors used for the Fabry-Perot interferometer, in conjunction with a single-pass loss (mainly due to reflection from the glass slides) of 20%. [The finesse is given by $F = \pi\sqrt{GR}/(1-GR)$].

The liquid crystal used was PCB. The film was 50- μm thick, and was oriented so that $\beta=22^\circ$. The Fabry-Perot cavity length was 4 cm, and the liquid-crystal film was placed at the position of minimum beam waist inside the cavity. By actual measurement, the fraction of laser power in the central spot (in the concentric interference rings intensity distribution) is 0.07 of the total laser power. The spot size of the laser on the film was estimated to be about $5 \times 10^{-4} \text{ cm}^2$.

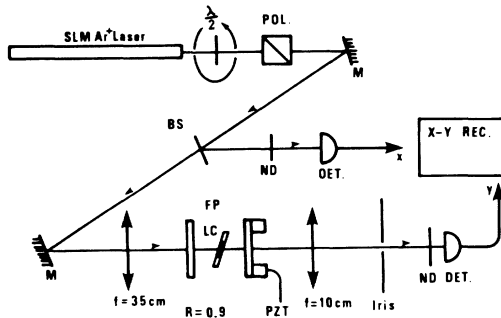


FIG. 2. Experimental arrangement: $\lambda/2$, half-wave plate; POL, linear polarizer; BS, beam splitter; FP, Fabry-Perot interferometer; LC, liquid-crystal film; pZT, computer-controlled piezoelectric transducer.

Before we proceed to describe the experimental result, we note here that for $\beta_2=22^\circ$, the thermal contribution to the nonlinearity ($\Delta n(\Delta T)$ is, from Eq. (27), given by $\Delta n(\Delta T) = \Delta n_1(\Delta T)[1 - (\delta + 1)\sin^2 22^\circ]$ is equal to $\Delta n_1(\Delta T)[1 - (\delta + 1)0.4]$. The liquid-crystal film was at room temperature,⁹ where $\delta \approx 5$. This gives $\Delta n(\Delta T) = 0.76\Delta n_1(T)$. Thus if the experiment were repeated for $\beta=0$, when thermal nonlinearity (for the same laser power) is given by $\Delta n_1(\Delta T)$, while the molecular reorientation contribution is vanishing, we will be able to estimate the thermal contribution, *if any*.

V. EXPERIMENTAL RESULTS AND COMPARISON WITH THEORY

The initial phase (with the laser at very low power) of the Fabry-Perot cavity was set with a step size of $0.05 \times 2\pi$ by the computer-controlled piezoelectric transducer. For $\phi_0=0, 0.1 \times 2\pi, -0.18 \times 2\pi$, we had observed the corresponding linear, differential gain and bistability operations in accordance with the theoretical predictions using these initial phase shifts. Each of the output-input scans took several minutes (i.e., very slow increase and/or decrease of the input laser was used). This is in view of the fact that nematic response time for a 50- μm sample is on the order of a few seconds. Figures 3(a)–3(c) depict the experimentally observed results corresponding to these ϕ_0 's. These modes of operation agree very well with the theoretical calculation based on the field-induced phase shift $\delta\phi$ [Eq. (13)] and the Fabry-Perot transmission η [Eq. (22)]. Bistability behavior was observed for the initial phase shift in the range of $-0.15 \times 2\pi$ to $-0.3 \times 2\pi$, again in good agreement with theory. For $\phi_0=0$, we have increased the incident power to more than 1 W. At these intensities, the scan showed some hysteresis which was probably due to laser heating at high intensity. If the incident power is increased to about 0.5 W and then reversed, no hysteresis was observed.

The agreement between theory and experiment is even more dramatic when we calculate the switching powers and the bistability curve and quantitatively compare them with the experimental results. For the theoretical calculation, we used $\phi_0 = -0.18 \times 2\pi$; $G=0.8$; thickness $d=50 \mu\text{m}$; $R=0.9$; $\beta_2=22^\circ$; $\Delta\epsilon=0.53$; $K=0.8 \times 10^{-7}$ cgs units.

Figure 3(d) shows the calculated bistability curve in a dotted line. Except for the overshoot (which cannot be obtained in a time-independent calculation), the agreement between the experimental results and the theory is excellent. The switch-up power was predicted to be 0.37 W (intensity 50 W/cm^2) while experimentally it was observed to be

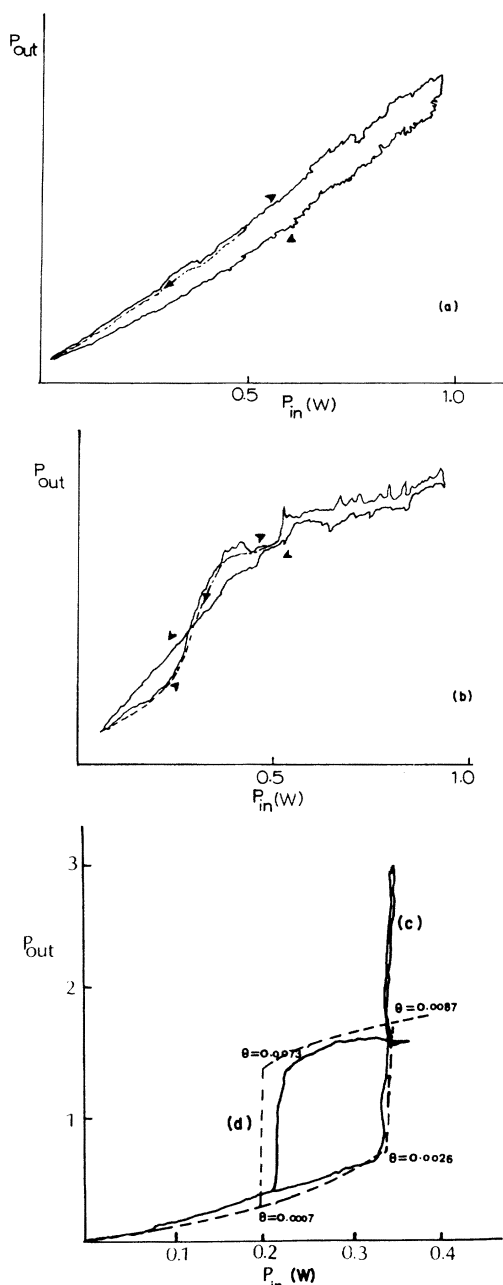


FIG. 3. (a) Output vs input power plot for an initial zero phase shift. The dotted line shows the curve if the laser power was reversed at 0.5 W, showing no hysteresis. The plot shows an expected linear dependence. (b) Output vs input power plot for an initial phase shift of -0.2 , showing a differential gain operation. Theoretical curve (not shown) also shows a differential gain mode for this phase shift. (c) and (d) Bistability in the output vs input plots [solid line (experimental)]. (d) shows the calculated theoretical curve in dotted line. Parameters used in the calculation are $\Delta\epsilon=0.56$, $K=0.8 \times 10^{-7}$ cgs units, $\beta=22^\circ$, film thickness is $50 \mu\text{m}$, $n_{||}=1.68$, $n_{\perp}=1.52$, $G=0.8$, $R=0.9$.

0.36 W. In estimating the switching intensity, we have taken into account that the laser power in the monitored central spot is 0.07 of the total laser power (as mentioned earlier). The switch-down power also agrees very well with the theoretical value.

The overshoot is due to the slow response of the molecule and consequently they are observable in the recording of the output beam. Typically, it takes about 3–4 sec for the whole overshoot to take place (i.e., an initial rise and a subsequent fall to a steady-state value). This “response” time is in agreement with the known response (reorientation) time of $50\text{-}\mu\text{m}$ -thick sample. The switch-off time was also noted to be of the same duration. We have also indicated in Fig. 1 the calculated molecular reorientation angle for the various points of interest. At switch up, for example, the angle θ changes from $\theta=0.0025$ rad to $\theta=0.009$ rad. These reorientation angles are very small (in justification of our earlier assumption in the calculation). However, when coupled to the large anisotropy of the nematics, these small reorientations are sufficient for providing the phase shift for bistability behavior.

Thermal contribution to the above observed phase effects was ruled out by the following simple experiment. The liquid-crystal film was oriented so that the plane of the film is perpendicular to the optical propagation, i.e., $\beta=0$. The incident laser power was then varied from 0 to 1 W, for various initial phase ranging from 0 to π . For all cases, a *straight linear output-input* curve was observed. Since thermal nonlinearity [in this case $\Delta n_{\perp}(\Delta T)$ for $\beta=0$] is larger than when the film is oriented with $\beta=22^\circ$, we conclude that thermal effects do not play any role in the bistability and other phase effects mentioned earlier for the case when $\beta=22^\circ$.

The orientation nonlinearity, as pointed out earlier, is dependent on $\sin 2\beta$. We have repeated the experiment for $\beta=11^\circ$, and we found that a much higher optical intensity (obtained by tighter focusing) is needed to see bistability. An intensity about *four times* that required to see switching for $\beta=22^\circ$ was required. At these intensities, the output after switch-on exhibits rather chaotic oscillations, and new (besides the original Fabry-Perot interference rings) spatial rings were observed (similar to those observed under self-focusing conditions). These wild oscillations may be the results of the combined effects of transverse modulations (due to self-focusing) and the Fabry-Perot’s longitudinal phase shift. The *total* intensity of the laser on the liquid crystal was about 2000 W/cm^2 and could have also induced thermal effects. This complicated situation

was clearly beyond a quantitative analysis. Nevertheless, in the case where $\beta=22^\circ$, these complications from thermal and/or self-focusing effects are not present and excellent agreements between experimental and theoretical results are obtained.

VI. CONCLUDING REMARKS

We have presented a detailed theoretical analysis of the optically induced phase shift in a nematic liquid-crystal film and the nonlinear Fabry-Perot transmission characteristics. The quantitative expressions derived here taking into account the *non-linear* and birefringent nature of the nematic film will serve as a useful reference for studying other similar light propagation problems (e.g., wave-front conjugation) since the problem is scarcely dealt with in the literature. The response of the nonlinear Fabry-Perot behavior is as expected. But what is interesting is that the large nonlinearity of the nematic

film enables us to use a low-power cw laser and *directly* (instead of inferring from pulsed laser time evolution) observe and compare the bistability behavior with theory. Within the range of power available in a cw laser, self-focusing and the associated transverse phase modulation effects can also be induced in the Fabry-Perot interferometer. These studies can obviously be also quantitatively carried out to provide further insights into optical bistability and other thin-film devices. They can also serve as a useful model for studying Gaussian beam intensity profile bistability.¹⁰

ACKNOWLEDGMENTS

This research is supported by a grant from the National Science Foundation under Contract No. ECS-80-26775. The experimental work was performed in the facilities of the National Research Council of Canada.

*Present address: Hua Zhong Institute of Technology, Wuhan, People's Republic of China.

¹See, for example, *Optical bistability*, edited by C. M. Bowden, M. Cifton, and H. R. Robl (Plenum, New York, 1980).

²See, for example, D. A. B. Miller, *Laser Focus* **18**, 79 (1982), and references therein. For a collection of recent papers, see also the special issue of *IEEE J. Quantum Electron.* **QE-17**, 300 (1981).

³H. M. Gibbs, S. L. McCall, and T. N. C. Venkatesan, *Phys. Rev. Lett.* **36**, 1135 (1976).

⁴F. S. Felber and J. H. Marburger, *Appl. Phys. Lett.* **28**, 731 (1976); *Phys. Rev. A* **17**, 335 (1978).

⁵T. Bischoffberger and Y. R. Shen, *Appl. Phys. Lett.* **32**, 156 (1976); *Phys. Rev. A* **19**, 1169 (1979).

⁶H. M. Gibbs, M. W. Derstine, F. A. Hopf, D. L. Kaplan, M. Rushford, R. L. Shoemaker, D. A. Weinberger, and W. H. Wing (unpublished).

⁷I. C. Khoo, R. Normandin, and V. C. Y. So, *J. Appl. Phys.* **53**, 7599 (1982).

⁸I. C. Khoo, *Phys. Rev. A* **25**, 1637 (1982).

⁹See, for example, K. C. Chu, C. K. Chen, and Y. R. Shen, *Mol. Cryst. Liq. Cryst.* **59**, 97 (1980).

¹⁰See, for example, W. J. Firth and E. M. Wright, *Opt. Commun.* **40**, 233 (1982).